JOURNAL OF SOLID STATE CHEMISTRY 120, 7–11 (1995)

Preparation and Crystal Structure of a New Praseodymium Manganese Germanate: $PrMnOGeO_4$

C. Gueho, D. Giaquinta, P. Palvadeau, and J. Rouxel[1]

Institut des Matériaux, Chimie des Solides, UM CNRS 110, 2, rue de la Houssinière, 44072 Nantes Cedex 03, France

Received February 10, 1995; accepted May 9, 1995

A new germanate, $PrMnOGeO_4$, was synthesized and its structure was determined from single crystal X-ray diffraction. $PrMnOGeO_4$ crystallizes in the triclinic space group $P\bar{1}$ with a = 5.636(1) Å, b = 5.706(1) Å, c = 6.941(1) Å, α = 106.14(1)°, β = 99.43(1)°, γ = 107.15(1)°, Z = 2, and R = 0.0252. The compound consists of infinite chains of staggered, *trans*-corner-sharing MnO_6 octahedra linked by GeO_4 tetrahedra in a distorted titanite structure. Channels between the chains of octahedra are filled with edge-shared units of 8-coordinate Pr. This new phase is described in the context of other chain compounds including titanite, KTP, and the $MOXO_4$ hydrates. Although the octahedral chains of $PrMnOGeO_4$ do not display the short manganese–oxygen contacts characteristic of the titanyl group in titanite and KTP, the formula is written as such for comparison with other compounds described in the literature.

INTRODUCTION

Compounds of stoichiometry $ABOXO_4$ (A = 6–8 coordinate alkali or alkaline earth metal, B = octahedrally coordinated metal, X = tetrahedrally coordinated element) crystallize in several related structure types containing infinite chains of corner-sharing octahedra cross-linked by corner-sharing tetrahedra. These structure types include the titanite structure ($CaTiOSiO_4$) (1, 2), the potassium titanyl phosphate structure ($KTiOPO_4$) (3–5), and various other $MOXO_4$ compounds such as $SbOPO_4$, which may contain a vacant or partially filled A-site (6, 7). These related structures—frameworks of interconnected octahedra and tetrahedra—belong to structure type 3 according to the systematic classification method of Bars *et al.* (8). This general structure type is described as having corner-sharing octahedral chains which are linked together by tetrahedra of which all corners are shared. Each tetrahedron thus is bound to four different octahedra, two of which belong to the same chain.

The major difference between the titanite structure and the KTP structure is the *trans–trans* arrangement of the staggered octahedral chains in titanite vs. the *cis–trans* arrangement in the KTP structure. Additional examples, such as β-$LiVOPO_4$ (9), contain eclipsed *trans–trans* octahedral chains (see Figs. 1a–1c). Most samples containing vacant or partially filled A-sites have the *trans–trans* staggered octahedral chains of the titanite structure. The majority of these structure types display alternating short–long metal–oxygen bonds in the octahedral chains. It is this structural feature which is believed to cause the second harmonic generation in KTP and the KTP-related compounds (5).

EXPERIMENTAL

Synthesis and Characterization Techniques

Single crystals of $PrMnOGeO_4$ were grown from the self-fluxing redox reaction described by the formula

$$PrCl_3 + MnCl_2 + \tfrac{3}{2}MnO_2 + GeO_2 \rightarrow PrMnOGeO_4 + \tfrac{3}{2}MnCl_2 + Cl_2.$$

Using a 1 mmole scale with a 10% molar excess of $MnCl_2$, reagent grade starting materials were sealed in a quartz tube and heated at 750°C for 5 days. The reaction mixture was washed with alcohol to free the metallic-appearing black platelets of $PrMnOGeO_4$ from the $MnCl_2$ flux. A JEOL JSM-35C scanning electron microscope equipped with a Tractor TN 5500 micro Z system was used for X-ray microanalysis. $Pr_3(SiO_4)_2Cl$ (10) was a common impurity resulting from attack on the silica tube. No silicon impurities were seen in crystals of $PrMnOGeO_4$, however.

Magnetic measurements were performed using a Quantum Design MPMS SQUID magnetometer. Polycrystalline samples were measured correcting for diamagnetic core corrections and the diamagnetic contribution of the gel-cap sample holder.

Structural Determination

Single crystals of $PrMnOGeO_4$ were analyzed by Weissenberg photography in order to select a nontwinned crystal suitable for structure determination.

[1] To whom correspondence should be addressed.

0022-4596/95 $12.00

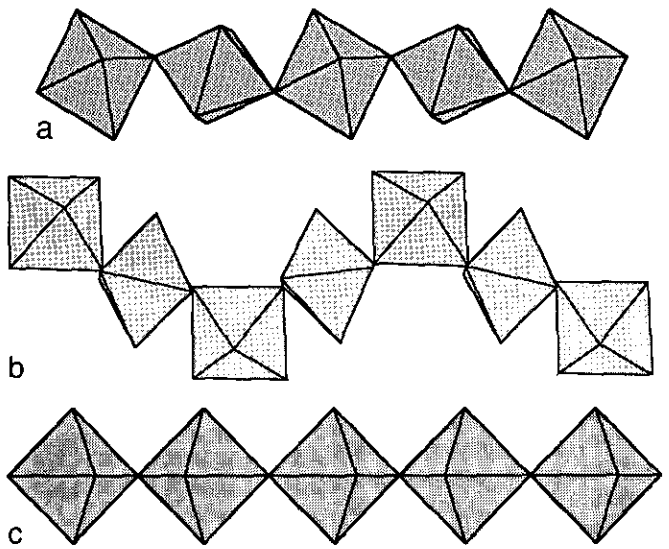

FIG. 1. (a) The staggered *trans–trans* arrangement of octahedral chains in the titanite structure. (b) The *cis–trans* arrangement of octahedral chains in the KTP structure. (c) The eclipsed *trans–trans* arrangement of octahedral chains in β-$LiVOPO_4$.

The cell parameters reported in Table 1 were determined and refined by diffraction techniques at 294 K with a least squares refinement based on 25 reflections with $4° \leq 2\Theta \leq 20°$. The data were collected using an Enraf–Nonius CAD4 diffractometer according to data collection parameters listed in Table 1. On the basis of Weissenberg photography, intensity statistics, and the successful solution and refinement of the structure, the space group of $PrMnOGeO_4$ was determined to be $P\bar{1}$ (No. 2). Data were corrected for Lorentz, polarization, absorption (11), and secondary extinction. Data reduction, structural solution, and refinement were performed using the SHELXTL PLUS (12) package of structural software. The atomic scattering factors were those of Cromer and Waber (13) and the corrections for anomalous dispersions were from Cromer and Waber (14). Positional and thermal parameters are listed in Table 2, while important interatomic distances and angles are listed in Table 3.

RESULTS AND DISCUSSION

1. Crystal Structure

The structure of $PrMnOGeO_4$ (Fig. 2) consists of infinite chains of staggered MnO_6 octahedra, corner-shared in a *trans–trans* fashion (Fig. 1a). These one-dimensional chains are interconnected by GeO_4 tetrahedra in the manner of structure type 3, as described by Bars *et al.* (8). $PrMnOGeO_4$ is the first example of a rare earth–manganese compound to crystallize in this general structure type. Bond–valence sums (15) for the Pr, Mn, Ge, and O

TABLE 1
Crystallographic Data and Experimental Details for $PrMnOGeO_4$

Empirical formula	$PrMnOGeO_4$
Formula weight (g/mol)	348.45
Crystal system	triclinic
Space group	$P\bar{1}$ (No. 2)
Lattice parameters:	
a (Å)	5.636(1)
b (Å)	5.706(1)
c (Å)	6.941(1)
α (°)	106.14(1)
β (°)	99.43(1)
γ (°)	107.15(1)
Volume (Å^3)	197.40
Z	2
Temperature (K)	294
Color and habit	black platelet
Crystal dimensions (mm)	0.12 × 0.07 × 0.02
D_{calc} (g/cm^3)	5.862
Diffractometer	Enraf–Nonius CAD4
Radiation	Mo $K\alpha$ (λ = 0.71073 Å)
$\mu_{(Mo\ K\alpha)}$ (cm^{-1})	227.6
Scan type	ω
F_{000}	312
$2\Theta_{max}$(°)	35
Quadrants measured (hkl)	±10, ±14, +11
No. of reflections measured	3698
No. observations ($I > 3.00\ \sigma(I)$)	1621
No. variables	77
Corrections:	
Lorentz polarization	
Absorption	
Secondary extinction	1.47(5) × 10^{-3}
Residuals: R; R_w	0.025; 0.022[a]
Goodness of fit indicator	1.42[b]
Largest peaks in final diff. map (e$^-$/Å^3)	+1.85, −1.74

[a] $R = \Sigma\|\|F_o| - |F_c\|/\Sigma|F_o|$ and $R_w = \Sigma(\|\|F_o| - |F_c\|\cdot\sqrt{w})/\Sigma(|F_o|\cdot\sqrt{w})$; $w = 1/\sigma^2(F_o)$.

[b] $S = \sqrt{[\Sigma(w\cdot\|F_o| - |F_c\|^2)/(M-N)]}$; M = # Observations; N = # Variables.

TABLE 2
Atomic Coordinates and U_{eq} Parameters for $PrMnOGeO_4$

Atom	Wyckoff	x	y	z	U_{eq}
Pr	2i	0.34856(5)	0.19066(5)	0.72257(4)	0.00613(8)
Mn1	1c	0	½	0	0.0048(3)
Mn2	1g	0	½	½	0.0054(3)
Ge	2i	0.30369(9)	0.16339(9)	0.23523(8)	0.0065(2)
O1	2i	0.0627(6)	0.1708(6)	0.3657(5)	0.007(1)
O2	2i	0.4220(6)	−0.2420(7)	0.5617(5)	0.009(1)
O3	2i	0.3227(6)	0.3685(6)	0.0904(5)	0.008(1)
O4	2i	0.2672(6)	−0.1497(6)	0.0783(5)	0.008(1)
O5	2i	0.0667(6)	0.4181(6)	0.7406(5)	0.008(1)

TABLE 3
Important Bond Lengths and Angles for $PrMnOGeO_4$

Atom	Atom	Å	Atom	Atom	Å
Pr	O1	2.678(4)	Mn1	O3 × 2	2.226(4)
	O1	2.452(3)		O4 × 2	1.978(3)
	O2	2.595(4)		O5 × 2	1.860(4)
	O2	2.566(4)		Mn2 × 2	3.470(1)
	O3	2.517(4)		Ge	3.428(1)
	O3	2.468(3)			
	O4	2.480(4)	Mn2	O1 × 2	2.012(4)
	O5	2.327(4)		O2 × 2	2.293(3)
	Mn1	3.475(1)		O5 × 2	1.866(4)
	Mn2	3.454(1)		Ge	3.317(1)
	Ge	3.307(1)			
	Pr*	4.116(1)	Ge	O1	1.755(4)
				O2	1.762(3)
				O3	1.735(4)
				O4	1.746(3)

Atom	Atom	Atom	°	Atom	Atom	Atom	°
O3	Mn1	O3	180	O1	Mn2	O1	180
O4	Mn1	O4	180	O2	Mn2	O2	180
O5	Mn1	O5	180	O5	Mn2	O5	180
O3	Mn1	O4	93.8(1)	O1	Mn2	O2	92.7(1)
O3	Mn1	O5	96.1(2)	O1	Mn2	O5	96.5(2)
O4	Mn1	O5	91.9(1)	O2	Mn2	O5	92.9(1)
Mn1	O5	Mn2	137.4(2)				
				O1	Ge	O2	102.9(2)
				O1	Ge	O3	110.4(2)
				O1	Ge	O4	114.0(2)
				O2	Ge	O3	116.8(2)
				O2	Ge	O4	102.3(2)
				O3	Ge	O4	110.3(2)

sites are in good agreement with their formal oxidation states at +3.01, +3.10, +3.99, and −2.02 valence units, respectively. The bond–valence value for the praseodymium site is uncharacteristic of this structure type in that the close agreement with the formal oxidation state implies a tightly bound site. This situation is unusual in comparison to other members of the general structure type where the *A*-cation is often only loosely bound; several examples exist in the literature for ion-exchange within these systems (3, 4, 16).

Additionally, the transition metal–oxygen chains in $PrMnOGeO_4$ lack the alternating short–long metal–oxygen bond lengths seen in other members of this general structure type. In $PrMnOGeO_4$ the octahedral chains are very regular in the *c*-direction; the bond lengths vary only slightly, 1.860(4) and 1.866(4) Å. This is in contrast to the bonding in both the titanite structure, 1.768(6) and 2.044(9) Å (2), and KTP, 1.718(4) and 2.161(4) Å (5). The lack of alternating short–long bond lengths has not been seen in any other compound in which the *B*-cation is a transition metal. The compounds $SbOPO_4$ and $KSbOSiO_4$, however, display bonding similar to that seen in $PrMnOGeO_4$ (6, 17). In $SbOPO_4$, the octahedral chain bond lengths are 1.903(3) Å × 2 (6), while in $KSbOSiO_4$, the octahedral chain bond lengths are 1.955(8) Å and 1.946(9) Å for Sb(1) and 1.96(1) Å and 1.961(9) Å for Sb(2) (17). The bonding similarity in the *B*-site between $SbOPO_4$ and $KSbOSiO_4$ must be assumed to be due to the presence of the nontransition metal antimony, as the phosphate crystallizes in the titanite structure with an empty *A*-site, while the silicate crystallizes in the KTP structure.

The triclinic structure of $PrMnOGeO_4$ is unusual within this general type; the more common crystal type is monoclinic with lattice parameters related to the general formulas calculated by Bars *et al.* (8). The triclinic cell of $PrMnOGeO_4$, however, may be transformed to an appropriate pseudo-monoclinic cell with lattice parameters of $a = 6.74$ Å, $b = 9.13$ Å, $c = 6.94$ Å, $\alpha = 94.2°$, $\beta = 111.9°$, and $\gamma = 90.7°$ according to the following matrix:

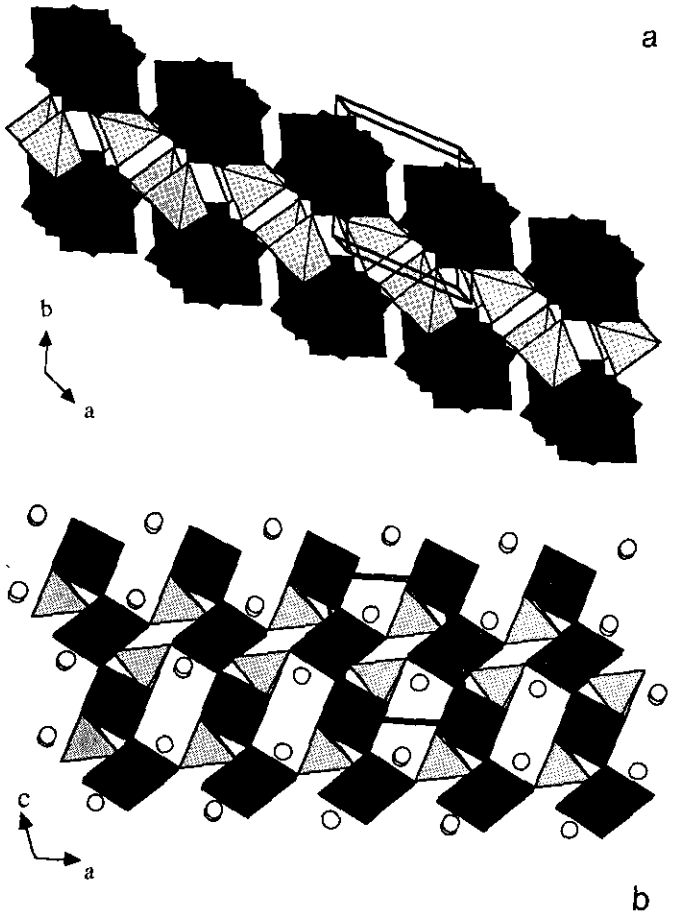

FIG. 2. The structure of $PrMnOGeO_4$ in (a) the *ab* plane and (b) the *ac* plane.

$$\begin{bmatrix} 1 & 1 & 0 \\ 1 & \bar{1} & 0 \\ 0 & 0 & \bar{1} \end{bmatrix}.$$

Although α is very distorted, this pseudo-cell may be used to contrast $PrMnOGeO_4$ with other monoclinic members of the structure type listed in Table 4. As can be seen in Table 4, the distortion in the pseudo-monoclinic cell of $PrMnOGeO_4$ results in a cell which has a larger *b*-parameter and a smaller β than is common. The major distortion is seen in $\alpha = 94.2°$. Chains of rare earth atoms run parallel to the *b*-axis in the pseudo-monoclinic cell; thus, the change in the *b*-parameter is perhaps due to the difference in the bonding of the rare earth site vs an alkali.

The differences in chain type between KTP and $PrMnOGeO_4$ can be rationalized through differences in the size of the *A*-cation. Phillips *et al.* compared similar differences between α-$NaTiOPO_4$ and KTP (4). In this case, the difference between *trans–trans* chains and *cis–trans* chains was reported to be due to the differences in the sizes of Na^+ and K^+. The more open framework of KTP provides 8- and 9-fold coordinate sites for K^+, while the structure of α-$NaTiOPO_4$ allows Na^+ to be in 6-fold coordination. Supporting the open framework idea of KTP are the calculated densities of α-$NaTiOPO_4$ and β-$NaTiOPO_4$ (isostructural with KTP), 3.36 and 2.94 g/cm^3, respectively. In $PrMnOGeO_4$, the more dense framework allows for tightly bound Pr, while the longer Ge–O bond lengths give the 8-fold coordination that the rare earth atom prefers.

2. *Magnetic Properties*

Figure 3 shows the temperature dependence (5–300 K) of the inverse of magnetization divided by applied field M/H for $PrMnOGeO_4$. The sample was first cooled in zero field and then measured upon heating in a field of 1 kG. The compound seems to retain paramagnetic behavior in the whole temperature range 5–300 K. In the range 100–300 K, the data are well described by a Curie–Weiss law with a Curie constant of $C = 4.66(2)$ emu K/mol and a paramagnetic Curie temperature $\theta_p = -18(1)$ K. The value of C leads to an effective moment of 6.10(2) μ_B/formula unit. This is similar to the theoretical value of 6.07 μ_B/formula unit calculated for Pr^{3+} cations in their lowest multiplet levels and Mn^{3+} cations in high spin states with spin-only contributions. Below 100 K, a deviation from the Curie–Weiss law of an uncertain origin occurs. This deviation might be attributable to the pres-

TABLE 4
Crystallographic Data of $PrMnOGeO_4$ and Related Structures

Compound	*a*(Å)	*b*(Å)	*c*(Å)	β(°)	Space group	Reference
$PrMnOGeO_4$	6.735	9.126	6.941	111.88	pseudo-$P2_1/c$	this paper
α-$LiVOPO_4$	6.748	7.922	7.206	116.99	pseudo-$P2_1/c$ ($P2_1/a$)	(20)
α-$NaTiOPO_4$	6.556	8.483	7.140	115.25	$P2_1/c$	(1)
$CaTiOSiO_4$	6.562	8.726	7.068	113.82	$P2_1/c$ ($P2_1/a$)	(2)
$NaVOAsO_4$	6.650	8.714	7.221	115.17	$P2_1/c$	(21)
$SbOPO_4$	6.791	8.033	7.046	115.90	$C2/c$	(6)

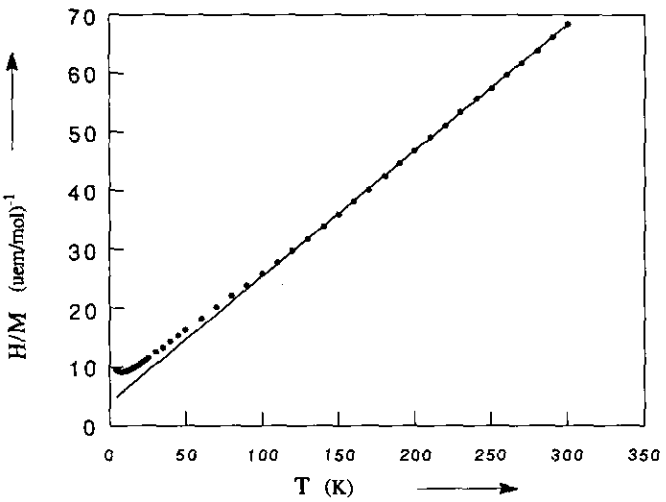

FIG. 3. The temperature dependence of the reciprocal susceptibility of $PrMnOGeO_4$ measured with a magnetic flux density of 1 kG. The line represents the high-temperature least-squares fit according to the Curie–Weiss law.

ence of antiferromagnetic interactions between Mn^{3+} cations. Alternatively, the paramagnetic properties of Pr^{3+} ions in a bicapped trigonal prism environment (Fig. 4) may also partly explain the low temperature behavior of M/H. Indeed, departures from the Curie–Weiss behavior are observed at low temperature for rare earth compounds (18, 19). These deviations are due to crystal field effects and do not reflect the presence of any magnetic interaction between the rare earth cations. A recent study of the experimental and the calculated magnetic susceptibilities of several Pr^{3+} compounds showed the susceptibilities to deviate from Curie–Weiss behaviors below ~100 K (19).

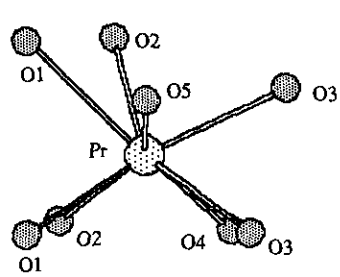

FIG. 4. The coordination of praseodymium in $PrMnOGeO_4$.

This deviation merges in a quasi-plateau in the reciprocal susceptibility plot at lower temperature (below 30–50 K). Such features are observed for $PrMnOGeO_4$ but the presence of paramagnetic Mn^{3+} makes it difficult to compare our experimental data with any kind of calculation. Furthermore, the decrease of susceptibility below ~10 K may be a genuine effect of antiferromagnetic interactions between the Mn^{3+} ions.

ACKNOWLEDGMENTS

The authors thank Y. Piffard and C. Payen for helpful discussions.

REFERENCES

1. C. R. Robbins, *Mater. Res. Bull.* **3,** 693 (1968).
2. M. Taylor and G. E. Brown, *Am. Mineral.* **61,** 435 (1976).
3. S. J. Crennell, R. E. Morris, A. K. Cheetham, and R. H. Jarman, *Chem. Mater.* **4,** 82 (1992).
4. M. L. F. Phillips, W. T. A. Harrison, G. D. Stucky, E. M. McCarron, J. C. Calabrese, and T. E. Gier, *Chem. Mater.* **4,** 222 (1992).
5. G. D. Stucky, M. L. F. Phillips, and T. E. Gier, *Chem. Mater.* **1,** 492 (1989).
6. Y. Piffard, S. Oyetola, A. Verbaere, and M. Tournoux, *J. Solid State Chem.* **63,** 81 (1986).
7. K. H. Lii, B. R. Chueh, H. Y. Kang, and S. L. Wang, *J. Solid State Chem.* **99,** 72 (1992).
8. O. Bars, J. Y. LeMarouille, and D. Grandjean, *Acta Crystallogr. Sect. B. Struct. Sci.* **37,** 2143 (1981).
9. K. H. Lii, C. H. Li, C. Y. Cheng, and S. L. Wang, *J. Solid State Chem.* **95,** 352 (1991).
10. P. Gravereau, B. Es-Sakhi, and C. Fouassier, *Acta Crystallogr. Sect. C. Cryst. Struct. Commun.* **44,** 1884 (1988).
11. A. North, D. Phillips, and F. Matthews, *Acta Crystallogr. Sect. A. Found. Crystallogr.* **24,** 351 (1968).
12. SHELXTL PLUS, Release 4. O. Siemens Analytical X-Ray Instruments, Madison, WI, 1989.
13. D. T. Cromer and J. T. Waber, *in* "International Tables for X-ray Crystallography," T. 2.2A. Kynoch Press, Birmingham, UK, 1974.
14. D. T. Cromer and J. T. Waber, *in* "International Tables for X-ray Crystallography," T. 2.3.1. Kynoch Press, Birmingham, UK, 1974.
15. N. E. Brese and M. O'Keefe, *Acta Crystallogr. Sect. B. Struct. Sci.* **47,** 192 (1991).
16. R. H. Jarman, *Solid State Ionics* **32/33,** 45 (1989).
17. M.-P. Crosnier, D. Guyomard, A. Verbaere, and Y. Piffard, *Eur. J. Solid State Inorg. Chem.* **27,** 845 (1990).
18. R. Saez Puche, M. Norton, T. R. White, and W. S. Glaunsinger, *J. Solid State Chem.* **50,** 281 (1983).
19. C. Cascales, R. Saez-Puche, and P. Porcher, *J. Solid State Chem.* **114,** 52 (1995).
20. A. V. Lavrov, V. P. Nikolaev, G. G. Sadlikov, and M. A. Porai-Koshits, *Sov. Phys. Dokl.* **27,** 680 (1982).
21. A. Haddad, T. Jouini, and Y. Piffard, *Eur. J. Solid State Chem.* **29,** 57 (1992).